Acta Mechanica 7, 1—15 (1969)

Approximate Solutions for the Structure of Shock Waves

By

M. R. Ananthasayanam and **R. Narasimha**, Bangalore, India

With 7 Figures

(Received January 26, 1968)

Summary — Zusammenfassung

Approximate Solutions for the Structure of Shock Waves. Approximate solutions of the B-G-K model equation are obtained for the structure of a plane shock, using various moment methods and a least squares technique. Comparison with available exact solution shows that while none of the methods is uniformly satisfactory, some of them can provide accurate values for the density slope shock thickness δ_n. A detailed error analysis provides explanations for this result. An asymptotic analysis of δ_n for large MACH numbers shows that it scales with the MAXWELL mean free path on the hot side of the shock, and that their ratio is relatively insensitive to the viscosity law for the gas.

Näherungsweise Lösungen für die Struktur von Stoßwellen. Unter Verwendung verschiedener Momentenmethoden und der Methode der kleinsten Quadrate werden Näherungslösungen der Gleichung des B-G-K-Modells für die Struktur eines ebenen Stoßes erhalten. Der Vergleich mit der verfügbaren exakten Lösung zeigt, daß zwar keine der Methoden durchwegs befriedigend ist, einige von ihnen aber genaue Werte für die Dichteanstiegs-Dicke δ_n des Stoßes liefern. Eine genaue Fehleruntersuchung gibt Erklärungen für dieses Ergebnis. Die asymptotische Analyse der Dicke δ_n für große MACHzahlen zeigt, daß sie mit der MAXWELLschen mittleren freien Weglänge auf der heißen Seite des Stoßes vergleichbar ist und daß der Quotient aus beiden verhältnismäßig unempfindlich gegen das Viskositätsgesetz des Gases ist.

1. Introduction

An exact solution of the BOLTZMANN equation for the structure of a plane shock layer is not yet available, and hence a large number of approximate methods [1, 2, 3] have been proposed. The simplest and most widely used of these is the moment method, in which a certain distribution function with one or more free parameters is assumed, and the parameter(s) evaluated by satisfying some moment of the BOLTZMANN equation. However, the result obtained often depends quite strongly on the moment function chosen; e. g., RODE and TANENBAUM [4] have studied the class of "power" moment functions $v_x{}^p$, where v_x is the com ponent of the molecular velocity along the direction of the flow, and found that different values of p lead to widely divergent values for the shock thickness.

Apart from this, there is no consistent or rational scheme for improving results from such approximate calculations. It is therefore very difficult to assess their value in a systematic way.

However, an exact solution of a model of the Boltzmann equation has been recently obtained numerically [5], and offers itself as a test case for the various approximate methods. The relative performance of these methods on the model equation could provide a guide for tackling the true Boltzmann equation. With this object in view, this paper presents approximate solutions of the B-G-K model equation, assuming the bimodal distribution of Mott-Smith with one free parameter. Various moment criteria, and a least squares method, are employed to evaluate the free parameter. As the restricted variational method of Rosen is essentially equivalent to the moment methods [6], it can also be considered as included in the present analysis.

Results for two of the moment functions considered by us here have recently been given by Quan [7]; but he does not present any comparison with the exact solution [5] for the problem. Anderson and Macomber [8] have also considered some moment methods for obtaining approximate solutions of the model equation. However the ansatz they employ for the distribution is rather more complicated than the usual bimodal, and has not been utilized in studies of the true Boltzmann equation. Hence it is not easy to relate the results of these workers to the approximate methods which have been employed till now on the true Boltzmann equation.

The fairly comprehensive analysis undertaken by the present work shows that while none of the methods considered is uniformly satisfactory, some of them are very successful for certain limited but important objectives, such as e. g. the prediction of the maximum density slope within the shock. A detailed analysis of the error distribution, in both velocity and physical space, is found to provide considerable insight into the nature of the different approximate methods, and convincing explanations for their relative success or failure; in particular, a critical assessment of the utility of the bimodal ansatz for the distribution function becomes possible. Based on these results, it is in fact possible to predict, with considerable confidence, the density slope shock thickness at sufficiently high Mach numbers. Further, an asymptotic analysis as the Mach number tends to infinity provides several new conclusions about the nature of the shock profile and dependence of the shock thickness on Mach number and the viscosity laws of the gas.

2. Description of Methods Used

For the one-dimensional problem of the flow through a plane, steady shock layer, we can write the Boltzmann equation as

$$v_x \frac{df(\mathrm{v}; x)}{dx} = \mathfrak{C}[f(\mathrm{v}; x)], \tag{2.1}$$

where f is the distribution function, x the coordinate along the mean flow, $\mathbf{v}$ the molecular velocity, v_x its component along x, and $\mathfrak{C}[f]$ the collision operator [9]. The boundary conditions on f are

$$f(\mathbf{v}; -\infty) = F_1(\mathbf{v}), \qquad f(\mathbf{v}; +\infty) = F_2(\mathbf{v}) \tag{2.2}$$

where

$$F = n(\beta/\pi)^{3/2} \exp\{-\beta(\mathbf{v}-\mathbf{u})^2\} \tag{2.3}$$

represents the MAXWELL distribution, and subscripts 1 and 2 indicate that the parameters in F correspond to the conditions far upstream and far downstream of the shock. These parameters are: n the number density, $\mathbf{u}$ the gas velocity and $\beta^{-1/2} = (2RT)^{1/2}$ the most probable thermal speed (R being the gas constant and T the temperature); and their values at $x = -\infty$ and $x = +\infty$ are related through the RANKINE-HUGONIOT equations.

Because of the complex nonlinearity of the collision operator $\mathfrak{C}$, an exact solution of (2.1) is in general difficult to obtain, even by purely numerical methods. In most approximate methods for strong shocks, the first step is to assume a form containing certain free parameters for f. In all the work reported here, we take this form to be bimodal following MOTT-SMITH [1] and write

$$f_{BM}(\mathbf{v}; x) \equiv [1 - \nu(x)] F_1(\mathbf{v}) + \nu(x) F_2(\mathbf{v}), \tag{2.4}$$

where ν is the parameter to be determined as a function of x. From (2.2) the boundary conditions on ν are

$$\nu(-\infty) = 0; \qquad \nu(+\infty) = 1. \tag{2.4a}$$

As (2.4) is not in general a solution of (2.1) it will lead to an "error" which we will define by

$$e(\mathbf{v}; \nu) \equiv v_x \frac{df_{BM}}{dx} - \mathfrak{C}[f_{BM}] = v_x (F_2 - F_1) \frac{d\nu}{dx} - \mathfrak{C}[f_{BM}]. \tag{2.5}$$

In the moment methods, $\nu(x)$ is chosen to make a certain weighted measure of the error (2.5) vanish, i. e. for some function $\Phi = \Phi(\mathbf{v})$ one puts

$$\int e(\mathbf{v}; \nu) \Phi(\mathbf{v}) \, D\mathbf{v} = 0, \tag{2.6}$$

where the integration covers the whole of the velocity space. It has been shown [6] that the restricted variational principle of ROSEN [2] is equivalent to making certain specific choices for $\Phi(\mathbf{v})$. Equation (2.6) represents a differential equation for ν:

$$\frac{d\nu}{dx}\left[\int v_x (F_2 - F_1) \Phi(\mathbf{v}) \, D\mathbf{v}\right] = \int \mathfrak{C}[(1-\nu) F_1 + \nu F_2] \Phi(\mathbf{v}) \, D\mathbf{v}. \tag{2.7}$$

Another possible method for obtaining ν is to minimize the error in some sense. For example, we may make a least squares estimate of ν by

requiring that the "total error" E^* given by

$$E^* = \int_{-\infty}^{+\infty} E\, d\,x, \qquad E \equiv \int e^2\,(\mathbf{v};\, v)\, D\mathbf{v} \tag{2.8}$$

be a minimum. (OBERAI [10] has recently proved an interesting result using this criterion). In the next section we obtain $v\,(x)$ for the B-G-K model equation by applying these two methods.

3. Approximate Solution for Model Equation

In the B-G-K model [11], the collision term is assumed to be given by

$$\mathfrak{C}\,(f) = A\, n\,(F - f), \tag{3.1}$$

where F is the local MAXWELLian distribution with the (unknown) parameters n, $\mathbf{u}$ and β which are given by

$$\begin{gathered} n = \int f\, D\mathbf{v}, \qquad n\,\mathbf{u} = \int f\mathbf{v}\, D\mathbf{v}, \\ 3\, n/2\, \beta = \int (\mathbf{v} - \mathbf{u})^2 f\, D\mathbf{v}. \end{gathered} \tag{3.2}$$

The number A can be considered to be a property of the gas, with the value [12]

$$A = c\, m/2\, \mu\, \beta, \tag{3.3}$$

where c is a constant, m is the mass of the molecule and μ is the viscosity. A unique choice for c is not possible as one cannot match both the viscosity and the thermal conductivity of a real gas with the model gas. The value $c = 1$ matches the viscosity and $c = 2/3$ matches the conductivity. In the shock structure problem where both are equally important a good average value for c may be taken as $5/6$. The variation of μ with temperature can be taken into account by making A depend suitably on the temperature. For simplicity we consider here only power law variations of the form $\mu \sim T^{\omega}$, where for most gases $1/2 < \omega < 1$, the limiting values corresponding respectively to rigid spheres and MAXWELL molecules.

3.1. Moment Equations

By putting the bimodal (2.4) in (3.2) we may obtain the ratios of n, u and T to their upstream values as functions of ν, γ (the ratio of the specific heats), and the upstream MACH number M_1; thus

$$n_{\xi 1} \equiv \frac{n\,(\xi)}{n_1} = (1 - \nu) + \nu\, u_{12} = u_{1\xi}, \tag{3.4}$$

$$T_{\xi 1} \equiv \frac{T\,(\xi)}{T_1} = \frac{(1 - \nu) + \nu\, T_{21}\, u_{12}}{n_{\xi 1}} + \frac{\gamma}{3}\, \frac{M_1^2\, u_{12}\,(1 - u_{21})^2\, \nu\,(1 - \nu)}{n_{\xi 1}^2}, \tag{3.5}$$

where the quantities with two subscripts denote the ratio of the quantity with the first subscript to the quantity with the second subscript (thus

$u_{12} = u_1/u_2$; $u_{\xi 1} = u(\xi)/u_1$), ξ being a nondimensional x coordinate defined as

$$\xi_1 = \frac{\pi}{4} \frac{x}{\Lambda_1} \tag{3.6}$$

and Λ_1 the MAXWELL mean free path in the upstream state,

$$\Lambda_1 = (5\pi/6)^{1/2} \frac{M_1 \mu_1}{n_1 m u_1}. \tag{3.7}$$

The relations (3.4) and (3.5) define the local MAXWELLian F in (3.1) and hence the collision term in the differential equation (2.7) can be evaluated in terms of ν, γ and M_1. Then for each choice of Φ we get a different differential equation (2.7). QUAN [7] studied the two choices $\Phi = v_x^2$, v_x^3 which have been employed by MOTT-SMITH [1] on the true BOLTZMANN equation. He found that for MAXWELL molecules ($\omega = 1$) the v_x^2 moment equations for the model and the true BOLTZMANN equation are identical and the v_x^3 equations differ by a constant numerical factor [7].

Apart from these "power" (polynomial) function moments one may choose other functions, such as exponentials. In this work we have chosen such exponential moments as $\Phi = F_1$, F_2 and $F_1 \pm F_2$. ROSEN's restricted variational principle is equivalent to using $\Phi = F_1 - F_2$ [13]. Equations for all these choices of Φ are listed in the Appendix.

3.2. Least Squares Solutions

Using (2.4) in (3.1) the error e defined in (2.5) becomes

$$e = v_x \nu' (F_2 - F_1) - A n (F - (1 - \nu) F_1 - \nu F_2), \tag{3.8}$$

where prime denotes differentiation with respect to x. Hence it can be easily seen that E in (2.8) van be expressed in the form of a quadratic expression in ν',

$$E = B_1 \nu'^2 + B_2(\nu) \nu' + B_3(\nu). \tag{3.9}$$

The function $\nu(x)$ which minimizes the total error E^* of (2.8) can be obtained as a solution of the EULER equation associated with the variational problem. Since E does not contain x explicitly this equation becomes

$$E - \nu' \frac{\partial E}{\partial \nu'} = 0, \tag{3.10}$$

using the boundary conditions (2.4a). Substituting (3.9) in (3.10) we get

$$\nu' = [B_3(\nu)/B_1]^{1/2}, \tag{3.11}$$

or in nondimensional form

$$\left(\frac{3\pi}{40}\right)^{1/2} \frac{d\nu}{d\xi_1} = \left(\frac{32}{\gamma}\right)^{1/2} n_{\xi 1} T_{\xi 1}^{(1-\omega)} (P/Q)^{1/2}, \tag{3.12}$$

where

$$P = [n_{\xi 1}^2\, T_{\xi 1}^{-3/2} + (1-\nu)^2 + \nu^2\, u_{12}^2\, T_{21}^{-3/2}]\, 2^{-3/2} +$$
$$+ 2\Big[\nu\,(1-\nu)\,u_{12}\,(1+T_{21})^{-3/2} \exp\Big\{-\frac{\gamma}{2} M_1^2 \frac{(1-u_{21})^2}{(1+T_{21})}\Big\} -$$
$$- (1-\nu)\, n_{\xi 1}\,(1+T_{\xi 1})^{-3/2} \exp\Big\{-\frac{\gamma}{2} M_1^2 \frac{(1-u_{\xi 1})^2}{(1+T_{\xi 1})}\Big\} -$$
$$- \nu\, u_{12}\, n_{\xi 1}\,(T_{21}+T_{\xi 1})^{-3/2} \exp\Big\{-\frac{\gamma}{2} M_2^2 \frac{(1-u_{\xi 2})^2}{(1+T_{\xi 2})}\Big\}\Big], \tag{3.13}$$

$$Q = (1+2\gamma M_1^2) + u_{12}^2\, T_{12}^{1/2}\,(1+2\gamma M_2^2) -$$
$$- \frac{4\,(8)^{1/2}\,(1+T_{21})^{-3/2}}{u_{12}\,(1+T_{12})}\Big[1+\gamma M_1^2 \frac{(1+T_{12}\,u_{21})^2}{(1+T_{12})}\Big] \cdot$$
$$\cdot \exp\Big\{-\frac{\gamma}{2} M_1^2 \frac{(1-u_{21})^2}{(1+T_{21})}\Big\}. \tag{3.14}$$

4. Results and Discussions

Since in general the first order ordinary differential equations (2.7) and (3.10) do not have simple closed form solutions, numerical integration is necessary to solve them. The integration can be started at some value of ν (which was 0.5 in our case) and continued towards either end. Using SIMPSON's rule with appropriate step sizes, the integration was carried out along both direction $x \to \pm\,\infty$ until a value of ν was reached where the numerical solution agreed with the asymptotic expression for the slope $d\nu/d\xi_1$. Beyond this value of ν, the asymptotic solution was used. The shock wave profiles were calculated at various MACH numbers for $\Phi = v_x^2,\ v_x^3,\ F_1,\ F_2,\ F_1 \pm F_2$ and with the least squares (LS) method. Most of the computations were made for a monatomic gas ($\gamma = 5/3$) with $\omega = 0.816$ (corresponding to Argon) and $c = 1$, so that the results could be directly compared with the exact solution of the problem by CHAHINE and NARASIMHA [5]. All computations were carried out on the Ferranti Sirius Computer at the National Aeronautical Laboratory, Bangalore.

4.1. Profiles and Error Analysis

It is well known (see e. g. [5]) that for $M_1 \lesssim 2$, the NAVIER-STOKES solution for shock structure is valid, and approximate methods of the kind we are discussing here become necessary only at higher MACH numbers. For this reason, we confine ourselves largely to a discussion of results at relatively large MACH numbers.

Fig. 1 compares density profiles obtained by various methods with the exact solution at $M_1 = 10$. Most of the approximate methods show fair agreement on the hot side of the shock, and reasonable to poor agreement on the cold side. The LS calculation shows excellent agreement around the middle of the shock but seems the poorest of the methods considered towards the cold side. It is also remarkable that the "exponential" moment

functions, F_1, F_2 and $F_1 \pm F_2$ show such good agreement over the middle of the shock.

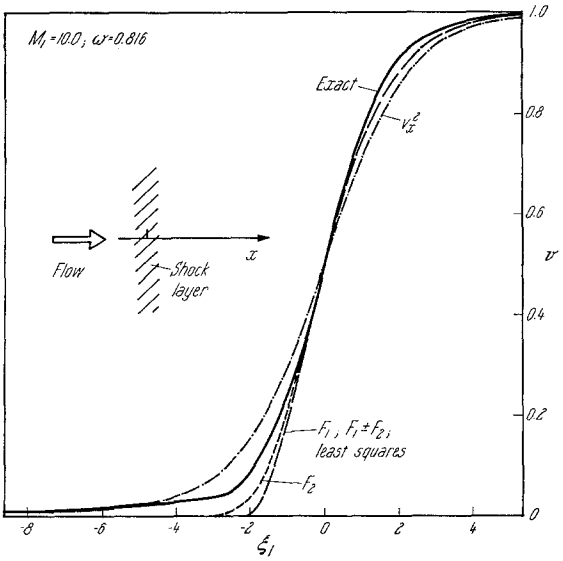

Fig. 1. Comparison of exact solution for the density profile [5] with approximate solutions by different methods. Solutions from moment methods are labelled by the moment function Φ used in the calculation. Note the close agreement between the exponential moments and the least squares results

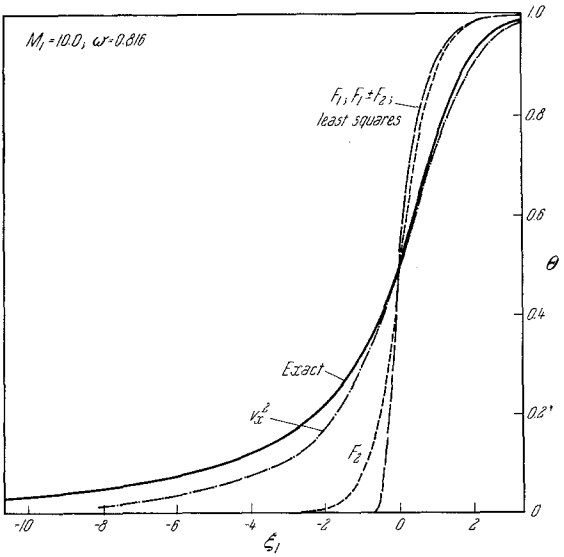

Fig. 2. Comparison of exact solution for the temperature profile [5] with approximate solutions by different methods

A comparison of the temperature profiles shown in Fig. 2, where $\theta \equiv (T_{\xi 1} - 1)/(T_{21} - 1)$, presents quite a different picture. The result

with $\Phi = v_x^2$ is closest to the exact solution, whereas the LS and the exponential moments give rather poor approximations.

It is thus immediately clear that none of the methods considered gives results which are uniformly good either in x or for all the moments. There are basically two reasons for this rather peculiar result. In the first place, the value (say θ^*) of θ at the location of maximum $dv/d\xi_1$ is fairly close to unity at large MACH numbers. For example, it can be shown from (3.5) that for a monatomic gas with $\omega = 1$, $\theta^* \simeq 0.8$ at $M_1 = 5$, and tends to 8/9 as $M_1 \to \infty$. (For $\omega < 1$, θ^* is even larger). Hence, the largest temperature gradient occurs at a smaller value of ν (i. e., further upstream) than that at which the maximum density gradient occurs. Consequently deviations noticed on the upstream side the shock in the density profile appear as deviations in the middle of the temperature profile! Similar results will obviously hold for higher moments of f.

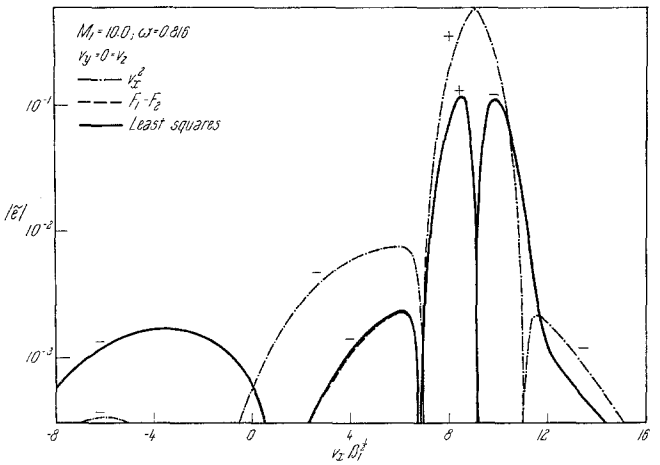

Fig. 3. Typical error distribution in velocity space. The + and − signs attached to the curves give the sign of e. The $F_1 - F_2$ curve is almost indistinguishable from the least squares curve

The second reason has to do with the nature of the approximate methods, and with the distribution of the error e defined by (2.5) as a function of x and v. Some representative error distributions are shown in Fig. 3 in which

$$\tilde{e} = \frac{4}{\pi} \frac{A_1 \pi^{3/2}}{n_1 \beta_1} e\,(v_x,\ 0,\ 0;\ \nu). \tag{4.1}$$

It is seen that at $\nu = 0.5$, around which most of the methods have their maximum density gradient, the LS and the $F_1 - F_2$ moment estimates show relatively small error over the whole velocity range, whereas the "power" moments v_x^2 and v_x^3 lead to larger errors. (In all these figures only v_x^2 results are displayed for reasons of clarity). The relative success of the exponential moments is also seen to be due to the relatively small weightage they give to the very high velocities, which contribute little

to the number density; thus the error is reduced in the most sensitive regions in velocity space. (In fact it is shown in the Appendix that in the limit as $M_1 \to \infty$, the LS, F_1 and the $F_1 \pm F_2$ moment estimates for the maximum density gradient are identical). In contrast, the weightage of the power moments is large at large velocities, which contribute little to the number density.

It was found that towards the hot side (e. g. at $\nu = 0.9$), the error plots for v_x^2, v_x^3, $F_1 - F_2$ and the LS methods which predict nearly the correct density slope have small error distribution over most of the velocity range. However towards the cold side (say $\nu = 0.1$), the v_x^2 and v_x^3 moments predict closer values to the exact than the least squares solution, although the latter has smaller local errors in velocity space.

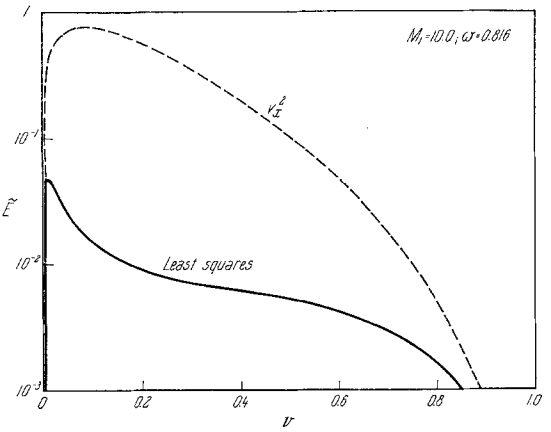

Fig. 4. Typical error distribution in physical space, showing how the least squares analysis results in errors less than a tenth of those in a v_x^2-moment calculation

The good performance of the LS technique in the middle of the shock and downstream of it, and its poor performance on the cold side, must be attributed to the assumed distribution function. It can be seen from Fig. 4 that the largest value of

$$\tilde{E} = \left(\frac{4}{\pi}\,\frac{\Lambda_1}{n_1}\right)^2 \frac{\pi^{3/2}}{\beta_1^{1/2}}\,E \tag{4.2}$$

occurs at quite small values of ν for all the methods. Further, one can minimize the local error E for a given ν (by choosing ν' so that $\partial E/\partial \nu' = 0$), instead of minimizing the integrated error E^*. It was found that even in this procedure, the largest error E occurs at small ν. It follows that the error which inevitably remains must be due to the inadequacy of the assumed distribution function on the cold side. This is further borne out in Fig. 5 which shows the ratio of the left to the right side in the BOLTZMANN equation (2.1) for the LS solution at various points inside the shock. At $\nu = 0.5$ and 0.9 this ratio is nearly unity over most of the velocity regions which contribute most to the number density. But at $\nu = 0.1$, this ratio

is seen to differ considerably from unity in wide regions of velocity space (especially for negative velocities), showing that even with minimum difference errors e, large percentage errors can remain. This indicates that the assumed bimodal distribution function is not adequate towards the cold side of the shock. There is also independent analytical support for this conclusion in the work of NARASIMHA [14] who has shown that the dominant feature of the distribution function on the cold side, especially for negative velocities, is a precursor from the hot side; this precursor distribution cannot be represented adequately as a sum of MAXWELLians, as assumed in the ansatz (2.4).

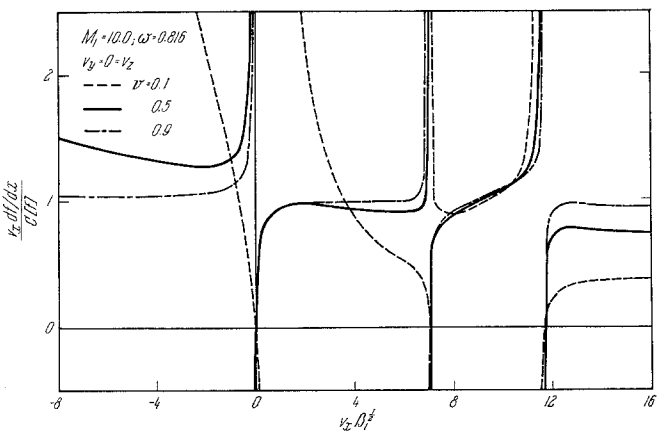

Fig. 5. Ratio of flow to collision term for the least squares solution. This ratio should be unity for the exact solution

The foregoing explanation of the results of the approximate calculations leads to an important conclusion. This is that at sufficiently high MACH numbers, the LS analysis and the exponential moments on the bimodal distribution should yield satisfactory values for the density slope shock thickness

$$\delta_n = (n_2 - n_1)/(dn/dx)_{\max}, \tag{4.3}$$

because these methods are quite accurate in the middle of the density profile of the shock, where the maximum density gradient occurs. On the other hand this must not be taken to imply that these methods give an adequate description of the complete density profile or of the profiles of higher moments of f. For example, if a temperature-slope shock thickness δ_T were to be defined in analogy with (4.3) the LS method as formulated here gives values of δ_T which are considerably in error!

4.2. Shock Thickness

Values of Λ_1/δ_n as obtained by all the methods considered here by us are shown in Fig. 6. They generally bear out the conclusion of the previous section; in particular the LS calculation is in excellent agreement with the exact results for $M_1 \gtrsim 5$. The exponential moments also agree

among themselves and with the exact solution for $M_1 \gtrsim 5$, but behave very differently as $M_1 \to 1$. It can be easily shown that this is due to differences in sign or in the orders of magnitude of either term of the differential equation (2.7), in the parameter $\epsilon \equiv M_1 - 1$ as $\epsilon \to 0$.

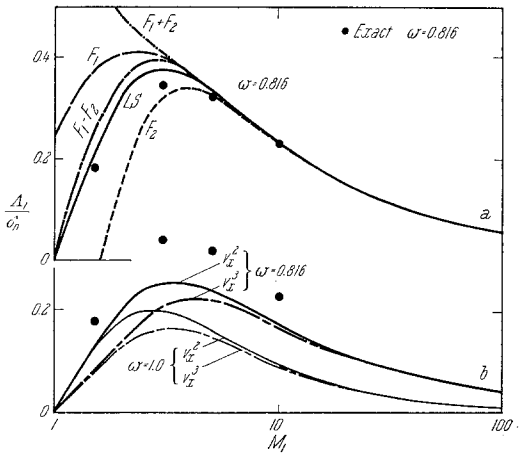

Fig. 6. The density slope shock thickness as calculated by different methods. The data in (a) show that all the exponential moments and the least squares result are very close to exact values for $M_1 \gtrsim 5$. Results in (b) show that the influence of ω is quite strong, and that the v_x^2, v_x^3 moments are generally inferior

The remarkable success of a class of approximate methods in predicting δ_n at sufficiently high MACH numbers along with the explanations provided by the error analysis, gives us sufficient confidence in them to be able to study the asymptotic behaviour of δ_n as $M_1 \to \infty$. Consider specifically the LS method. Equation (3.12) becomes, in the limit ν fixed, $M_1 \to \infty$,

$$\left(\frac{3\pi}{40}\right)^{1/2} \frac{d\nu}{d\xi_1} = \frac{3(1+3\nu)}{5 M_1} \left[\frac{8\nu(1+\nu)}{(1+3\nu)^2}\right]^{(1-\omega)} \left(\frac{5 M_1^2}{16}\right)^{(1-\omega)} (1-\nu), \quad (4.4)$$

for a monatomic gas. This equation is not strictly valid in the limit $\nu \to 0$. However (4.4) provides a good approximation where $\nu = 0\,(1)$, and in particular in the region where $d\nu/d\xi_1$ is a maximum, so that it is sufficiently accurate for obtaining δ_n.

It may be seen from the above differential equation that $d\nu/d\xi_1$ is proportional to $M_1^{(1-2\omega)}$ as $M_1 \to \infty$. From (3.7) the ratio of the MAXWELL mean free path on the cold side to that on the hot side is also of the same order. Hence the shock thickness would be finite in terms of a length scale referred to the hot side mean free path, Λ_2; and Equation (4.4) can be written as

$$\left(\frac{3\pi}{40}\right)^{1/2} \frac{d\nu}{d\xi_2} = \frac{3(5)^{1/2}(1+3\nu)}{16} \left[\frac{8\nu(1+\nu)}{(1+3\nu)^2}\right]^{(1-\omega)} (1-\nu), \quad (4.5)$$

$$\xi_2 \equiv \xi_1 \Lambda_1/\Lambda_2. \quad (4.6)$$

MUCKENFUSS [15] has also obtained the same asymptotic dependence of maximum $dv/d\xi_1$ on M_1, but he scales the shock thickness with a mean free path Λ_0 defined somewhere in the middle of the shock. As the state of the gas at such a point is known only from an approximate solution for the shock structure, Λ_0 is not uniquely defined. Our choice of Λ_2 as the scaling length has the advantage that its value can be determined independently of the uncertainties in the method of solution.

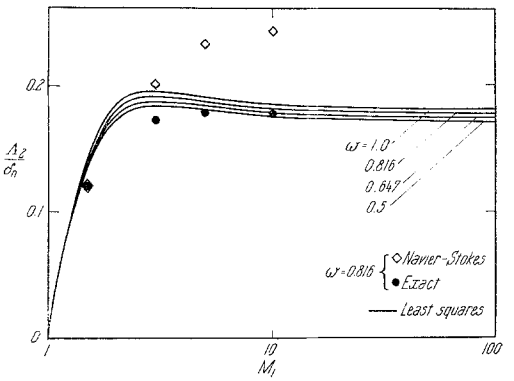

Fig. 7. Density slope shock thickness in terms of the MAXWELL mean free path on the hot side of the shock. Note the weak dependence of the results on ω

Results for Λ_2/δ_n obtained from (3.12) are shown in Fig. 7, a striking feature of which is that the influence of ω is relatively weak. The physical reason for this is as follows. At and beyond the point where $dv/d\xi_1$ is a maximum, the temperature is already quite close to the hot side value for all ω, as we have previously remarked. (In any case, (3.5) shows that for $v = O(1)$, we have $T = O(T_2)$.) Hence in this region the variation in the mean free path is due largely to variations in the density, and so will be nearly the same for all ω. We may therefore expect the density profiles, and in particular the maximum density slope, to be relatively insensitive to ω (or more generally, to the viscosity law) if Λ_2 is used as the scaling length. It is interesting to note that in this region the mean free path must decrease towards its hot side value, as the density increases and the temperature is nearly constant. Thus the MAXWELL mean free path Λ attains a maximum value somewhere within the shock. However the profiles upstream of the maximum density gradient may be expected to be different for different gases, due to the large variation in this region of the mean free path with temperature. This variation is stronger for larger values of ω, and hence the asymmetry in the density profiles may be expected to increase as $\omega \to 1$. This fact has been predicted by LIEPMANN, NARASIMHA and CHAHINE [16] based on purely dimensional considerations.

It is interesting that in the limit $M_1 \to \infty$, the results predicted by the moment methods using $\Phi = F_1$, $F_1 \pm F_2$ are identical with those of

the LS method. It is shown in the Appendix that the differential equations for these moment methods, in the limit ν fixed, $M_1 \to \infty$, are the same as (4.4).

5. Conclusion

It has been shown that none of the approximate methods considered can be relied upon to give the complete profile of even the first few moments of the distribution satisfactorily. On the other hand, for the limited but important objective of obtaining the density slope thickness of the shock, there are sound reasons (based on a detailed error analysis) for preferring certain moment methods, particularly those involving exponentials, and a least squares criterion; and these methods show good agreement with exact results when $M_1 \gtrsim 5$. Further, the MAXWELL mean free path on the hot side is the appropriate scaling length for the density-slope thickness, and with its use results become much less sensitive to the viscosity law. In a separate note, it will be shown that similar results hold for the true BOLTZMANN equation.

Appendix

The nondimensional form of the differential equations for the moments F_1, F_2 and $F_1 \pm F_2$ can be written as

$$\left(\frac{3\pi}{40}\right)^{1/2} \frac{d\nu}{d\xi_1} = \frac{2(\gamma-1)}{(3-\gamma)} \frac{u_{12}(1-u_{21})^2}{3(T_{21}-1)} M_1 \nu (1-\nu) T_{\xi 1}^{(1-\omega)};$$

$$\Phi = v_x^2, \tag{A 1}$$

$$= \frac{(3+\gamma M_1^2) - T_{21}(3+\gamma M_2^2)}{M(1) - u_{12} T_{21}^2 M(2)} (u_{12}-1) M_1 \nu (1-\nu) T_1^{(1-\omega)};$$

$$\Phi = v_x^3, \tag{A 2}$$

$$= \chi \frac{G_1}{G_2}; \qquad \Phi = F_1, \tag{A 3}$$

$$= \chi \frac{G_3}{G_4}; \qquad \Phi = F_2, \tag{A 4}$$

$$= \chi \frac{G_1 \pm u_{12} T_{12}^{3/2} G_3}{G_2 \pm u_{12} T_{12}^{3/2} G_4}; \qquad \Phi = F_1 \pm F_2, \tag{A 5}$$

where

$$M(i) = 3 + 6\gamma M_i^2 + \gamma^2 M_i^4, \qquad i = 1,2$$

$$\chi = \frac{n_{\xi 1} T_{\xi 1}^{(1-\omega)}}{\gamma M_1},$$

$$G_1 = n_{\xi 1} E_{\xi 1} - (1-\nu) E_{11} - \nu u_{12} E_{21},$$

$$G_2 = \frac{1 + T_{21} u_{12}}{1 + T_{12}} E_{21} - E_{11},$$

$$G_3 = n_{\xi 1} E_{\xi 2} - (1 - \nu) E_{12} - \nu u_{12} E_{22},$$

$$G_4 = \frac{1 + T_{12} u_{21}}{1 + T_{12}} E_{12} + E_{22},$$

and

$$E_{ij} = \left[\exp - \frac{\beta_i u_i^2 (1 - u_{ji})^2}{(1 + \beta_{ij})}\right] (1 + \beta_{ji})^{-3/2}, \; i, j = \xi, 1, 2. \qquad \text{(A 6)}$$

From (3.5), it is seen that $T_{\xi 1} \to \infty$ for fixed ν, as $M_1 \to \infty$. Using this fact it is easy to show that the asymptotic form of the differential equations (A 3), (A 4) and (A 5) is identical with that obtained by the least squares method, namely (4.5). Alternatively, multiplying (2.5) by DIRAC's delta function $\delta(\mathbf{v} - \mathbf{u}_1)$ and integrating over the whole velocity space leads to (4.5). Also if one notes that $E_{\xi 2}$ and $T_{\xi 2}$ are very nearly unity as $M_1 \to \infty$ over most of the region in ν, then the differential equation for F_2 also becomes identical to (4.4).

The asymptotic form of the v_x^2 and v_x^3 moment differential equations are identical:

$$\left(\frac{3\pi}{40}\right)^{1/2} \frac{d\nu}{d\xi_1} = \frac{12}{5 M_1} \nu (1 - \nu) T_{\xi 1}^{(1-\omega)}. \qquad \text{(A 7)}$$

References

[1] MOTT-SMITH, H. M.: The solution of the BOLTZMANN equation for a shock wave. Phys. Rev. **82**, 885–892 (1951).

[2] ROSEN, P.: The solution of the BOLTZMANN equation for a shock wave using Restricted Variational Principle. Jour. of Chem. Phys. **22**, 1045–1049 (1954).

[3] GLANSDORFF, P.: The thickness of shock waves by the two fluid model theory extended to rarefied gases. 2nd International Symposium on Rarefied Gas Dynamics, Berkeley, California, 475–478 (1960).

[4] RODE, D. L. and S. B. TANENBAUM: MOTT-SMITH shock thickness calculations using the v_x^p method. Phys. Fluids, **10**, 1352 (1967).

[5] CHAHINE, M. T. and R. NARASIMHA: Exact numerical solution of the complete B-G-K equation for strong shock waves. 4th International Symposium on Rarefied Gas Dynamics, Toronto, 140–160 (1964).

[6] NARASIMHA, R.: Moment methods and "Restricted Variation" in kinetic theory. Phys. Fluids, **9**, 2524–2525 (1966).

[7] QUAN, V.: Solution for a shock wave of Bimodal Distribution using BHATNAGAR-GROSS-KROOK models. Phys. Fluids, **10**, 889–891 (1967).

[8] ANDERSON, D. G. and H. K. MACOMBER: Numerical experiments in kinetic theory. 4th International Symposium on Rarefied Gas Dynamics, Toronto, 96–111 (1964).

[9] CHAPMAN, S. and T. G. COWLING: The Mathematical Theory of non-uniform gases. 2nd Edn. p. 63. Cambridge Univ. Press, London and New York (1953).

[10] OBERAI, M. M.: MOTT-SMITH Distribution and Solution of Kinetic Equations. Journal de Mécanique, **6**, 317 (1967).

[11] BHATNAGAR, P. L., E. P. GROSS and M. KROOK: A model for collision processes in gases. Phys. Rev. **94**, 511 (1954).

[12] LIEPMANN, H. W., R. NARASIMHA and M. T. CHAHINE: Structure of a plane shock layer. Phys. Fluids, **5**, 1313–1324 (1962).

[13] GUSTAFSON, W. A.: On the BOLTZMANN equation and the structure of shock waves. Phys. Fluids, **3**, 732–734 (1960).

[14] NARASIMHA, R.: Asymptotic solutions for the distribution function in non-equilibrium flows. I. J. Fluid Mech., **34**, 1—24 (1968).
[15] MUCKENFUSS, C.: Some aspects of shock structure according to the bimodal model. Phys. Fluids, **11**, 1325—1336 (1962).
[16] LIEPMANN, H. W., R. NARASIMHA and M. T. CHAHINE: Theoretical and experimental aspects of the shock structure problem. Eleventh International Congress on Applied Mechanics, Munich, 973—979 (1964).

M. R. Ananthasayanam and R. Narasimha
Technical Assistant and Associate Professor, respectively
Department of Aeronautical Engineering
Indian Institute of Science
Bangalore-12, India